6404–6417 *Nucleic Acids Research, 2010, Vol. 38, No. 19* *Published online 11 June 2010*
doi:10.1093/nar/gkq504

Binding site number variation and high-affinity binding consensus of Myb-SANT-like transcription factor *Adf-1* in Drosophilidae

Michael Lang and Elvira Juan*

Departament de Genètica, Universitat de Barcelona, 08028 Barcelona, Spain

Received March 26, 2010; Revised May 17, 2010; Accepted May 19, 2010

ABSTRACT

There is a growing interest in the evolution of transcription factor binding sites and corresponding functional change of transcriptional regulation. In this context, we have examined the structural changes of the ADF-1 binding sites at the *Adh* promoters of *Drosophila funebris* and *D. virilis*. We detected an expanded footprinted region in *D. funebris* that contains various adjacent binding sites with different binding affinities. ADF-1 was described to direct sequence-specific DNA binding to sites consisting of the multiple trinucleotide repeat $[G^{C}/_{T}\,^{C}/_{T}]_{4-5}$. The ADF-1 recognition sites with high binding affinity differ from this trinucleotide repeat consensus sequence and a new consensus sequence is proposed for the high-affinity ADF-1 binding sites. *In vitro* transcription experiments with the *D. funebris* and *D. virilis* ADF-1 binding regions revealed that stronger ADF-1 binding to the expanded *D. funebris* ADF-1 binding region only moderately lead to increased transcriptional activity of the *Adh* gene. The potential of this regional expansion is discussed in the context of different ADF-1 cellular concentrations and maintenance of the ADF-1 stimulus. Altogether, evolutionary change of ADF-1 binding regions involves both, rearrangements of complex binding site cluster and also nucleotide substitutions within sites that lead to different binding affinities.

INTRODUCTION

There is increasing interest in the understanding of sequence evolution of non-coding DNA. It has long been claimed that phenotype diversification among species does not only involve alterations of biochemical properties of translated gene products, but also depends much more on differentiations of spatiotemporal expression of genes within a tissue or throughout the whole organism (1). Numerous studies have supported that mutations within *cis*-regulatory regions underlie a variety of phenotypic differences in morphology and physiology (2,3).

A problem in the understanding of *cis*-regulatory sequence evolution is that few general rules have been elucidated yet to relate it to functional evolution of gene expression (4,5). Inter-specific sequence comparisons of non-coding DNA reveal conserved regions and many of them likely are *cis*-regulatory elements (6–11). But despite obvious indications of selective constraint the structure and sequences of *cis*-regulatory modules change over time, even in cases where expression patterns are conserved. For example, the stripe pattern expression of the pair rule gene '*even-skipped*' (*eve*) is highly conserved in Drosophila. However, the functional analysis of the *eve* stripe 2 enhancer revealed functional differences between closely related species and functional convergence between distantly related species (5,12,13) and it was proposed that stabilizing selection has not only maintained phenotypic constancy of *eve* gene expression, but also allowed mutational turnover of functionally important sites within the stripe 2 enhancer.

A future approach to comprehensively understand the relationship between *cis*-regulatory DNA sequences and gene transcription might therefore be the establishment of a framework of quantitative probabilistic models (14,15). However, crucial information is still needed to be implemented for a realistic prediction of transcriptional outputs.

Although high-throughput approaches more rapidly gain data of protein–DNA interactions and binding preferences of transcription factors, the investigation of case studies is justified because high-throughput methods are often not sensitive enough for special characteristics of selected components. For example, transcription factors often recognize multiple distinct sequence motifs (16) that might be better resolved in more meticulous

*To whom correspondence should be addressed. Tel: +34 934021496; Fax: +34 934034420; Email: ejuan@ub.edu

small-scale experimental approaches. Overall, the understanding of transcriptional regulation and its evolutionary diversification among species requires a detailed knowledge of DNA–protein interactions of every transcription factor involved. It is therefore desirable to focus on the analysis of regulatory changes of well-studied genes for which experimental data exist.

The *Adh* gene expression and transcriptional regulation of *Drosophila melanogaster* have been intensively studied and several regulatory mechanisms have been proposed to account for differential *Adh* transcription in a characteristic spatiotemporal pattern (17–29).

The transcription factor ADF-1 binds among other genes at the distal and proximal regulatory promoters of the *Adh* gene of *D. melanogaster*. While ADF-1 activates *Adh* transcription through binding at the distal promoter, the function of the interaction at the proximal promoter has remained unclear (27,30). The *Adh* proximal promoter region is partially conserved in a wide range of Drosophilidae species and putative ADF-1 binding sites are detected. In *D. funebris*, the *Adh* gene lacks the distal promoter and its regulatory promoter is diverged compared with other species of the subgenus Drosophila such as *D. virilis* (31,32). We have studied the interaction of ADF-1 with the *D. funebris Adh* regulatory promoter, its binding preferences, site diversification and functional contribution to *Adh* transcription. We show that ADF-1 binds to multiple adjacent recognition sites within an expanded ADF-1 binding region at the *D. funebris Adh* regulatory promoter. ADF-1 contains a Myb/SANT-like DNA binding domain of approximately 80 amino acids that was described to direct sequence-specific DNA binding to a site consisting of multiple trinucleotide repeats. The ADF-1 binding consensus was described as a $[G^C/_T C^C/_T]_{4-5}$ repeat sequence (33). However, we found that high-affinity ADF-1 binding sites do not match this consensus and have proposed a new binding consensus. Although regions with more adjacent binding sites revealed also increased ADF-1 binding *in vitro*, only moderatedly higher activation of *Adh* transcription was observed. We speculate that different regional expansions of ADF-1 binding site clusters might result in differential response to varying cellular ADF-1 concentrations, similarly to what had been suggested for homotypic binding site clusters, scattered over larger genomic regions (34,35). Therefore, not only the nucleotide substitutions but also gains and losses of recognition sites are important in the evolution of the ADF-1 binding regions.

MATERIAL AND METHODS

Expression and purification of ADF-1

ADF-1 was expressed in BL21 cells (Novagen) with *Adf-1* coding sequences of *D. melanogaster* (GenBank accession number NM206028), *D. funebris* (GQ922007) and *Scaptodrosophila lebanonensis* (AJ538295) cloned into the pASKIBA37p expression vector (IBA) and N-terminal His-tagged ADF-1 was purified from inclusion bodies from 1-l liquid culture after 4 h induction at RT, following Gaul *et al.* (36) with some modifications. Inclusion body precipitate was dissolved in 20-ml denaturation buffer (250 mM HEPES, 500 mM NaCl, 1 mM EDTA, 8 M urea, pH 8) and dialyzed twice for 2 h in 1 l of dialysis buffer (50 mM HEPES, 0.5 M NaCl, 40 mM imidazole, 10% glycerol, pH 8.0). ADF-1 was purified from renaturaded protein solutions with a 1-ml His-trap FF column (GE Healthcare).

In vitro DNA binding assays

Labeling of DNA fragments for electromobility shift assay (EMSA) was obtained by PCR either by α^{32}P dCTP incorporation or with end-labeled oligonucleotides (37). Labeling of DNA fragments of the EMSA shown in Figure 1 was carried out by PCR with 2.5 mM dATP, dTTP, dGTP, 0.25 mM dCTP and variable amounts of α^{32}P dCTP. For equal labeling of the different fragments, the amounts of α^{32}P dCTP were adjusted to a ratio α^{32}P dCTP/cold dCTP that in average led to one incorporation of α^{32}P dCTP per double-stranded DNA molecule. PCR products were purified by excision from 7% acrylamide gels (1× TBE: 89 mM Tris, 89 mM boric acid, 10 mM EDTA; pH 8.3) followed by electroelution in dialysis tubes and phenol:chloroform extraction.

EMSA binding reactions were performed with 2–70 fmol labeled DNA mixed with 12.5 ng sheared salmon sperm (unspecific competitor DNA) per microliter reaction volume, 0.5 volumes of 2× binding buffer I (65 mM HEPES pH 7.6, 0.1 mM EDTA, 12.5 mM $MgCl_2$, 1 mM DTT, 10% glycerol, 100 mM KCl) or 2× binding buffer II (20 mM Tris pH 7.9, 0.2 mM EDTA, 8 mM $MgCl_2$, 100 mM NaCl, 9% Ficoll 400, 100 μg/ml BSA, 0.4% NP-40, 2 mM DTT) and purified ADF-1 (0–200 ng). Binding reactions were incubated for 15 min at 23°C. Samples were loaded on a 7% acrylamide gel in 0.5× TBE and 0.05% NP-40 and electrophoresis was carried out at 400 V for 2 min and 200 V for 1–2 h in 0.5× TBE buffer (44.5 mM Tris, 44.5 mM boric acid, 5 mM EDTA; pH 8.3).

DNase I footprinting binding reactions were carried out in binding buffer I with 6 fmol end-labeled DNA 0–150 ng ADF-1, for 20 min at 23°C. Reactions were mixed with 20 μl of diluted DNase I (10 mM $MgCl_2$, 20 mM $CaCl_2$, 1.5–6 ng DNase I) and incubation was stopped after 30 s at 23°C with addition of 40 μl stop solution (0.3% SDS, 15 mM EDTA, 600 mM Na acetate, 250 μg/ml yeast tRNA, 15 μg/ml proteinase K). Phenol:chloroform extracted samples were run on 5% sequencing gels. G+A chemical sequencing DNA ladder was applied to each gel.

For the methylation interference assay, end-labeled DNA fragments were partially methylated (approximately one methylated guanine per DNA molecule) with dimethylsulfate (DMS) as described in Carey and Smale (38). Preparative EMSA experiments were carried out with 300–400 fmol of end-labeled and partially methylated DNA and 1.5–2 μg ADF-1. After electrophoresis the bands of shifted and free DNA were excised and purified by electroelution and phenol:chloroform extraction. Precipitated DNA was resuspended in 1 M piperidine and was incubated for cleavage for 30 min at 90°C, followed by four rounds of freeze drying with dry ice

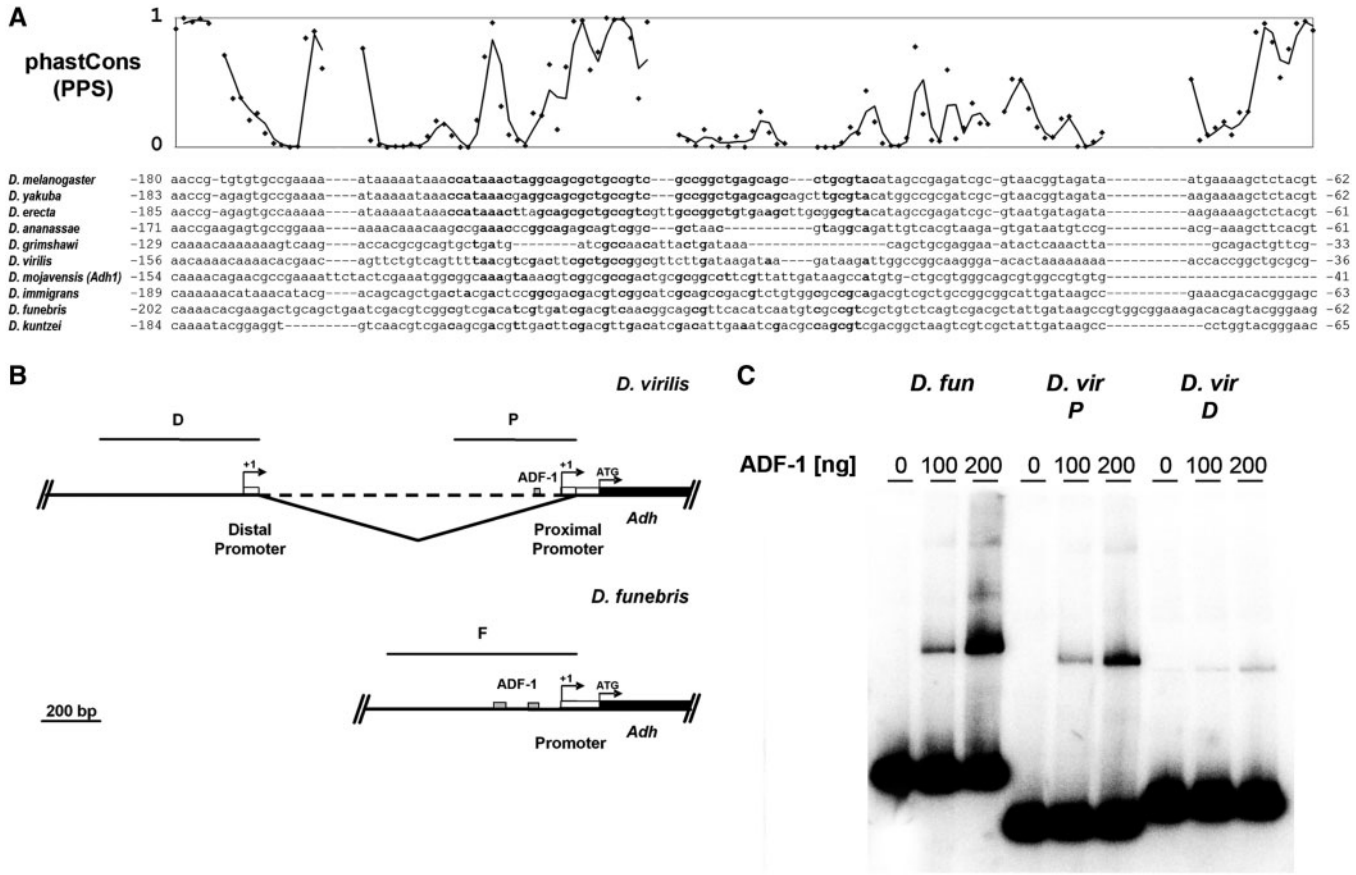

Figure 1. ADF-1 binding sites at the *Adh* proximal promoter. (**A**) Conservation evaluation with phastCons (61). Conservation estimates are indicated by diamonds, the line shows the moving average. (**B**) Putative ADF-1 binding sites in the *Adh* promoter regions of *D. virilis* (43) and *D. funebris* (32), indicated by gray boxes (**C**) EMSA with corresponding promoter regions, using *S. lebanonensis* ADF-1. P: *D. virilis* proximal promoter, D: *D. virilis* distal promoter, D. vir: *D. virilis*, D. fun: *D. funebris*.

and a speed vac (Heto), and resuspension in 10 µl ddH_2O. Equal amounts of each sample (10 000–15 000 cpm) were run on a 7% sequencing gel.

Chromatin immunoprecipitation

An anti-ADF-1 antibody was purified from rabbits, immunized with four boosts of 400 µg ADF-1. The antibody was purified by affinity chromatography from serum using recombinant ADF-1, with Gln residues 129–136 substituted by three Ala residues in order to remove a redundant epitope in the *trans*-activation domain. A total of 5-mg modified ADF-1 was coupled to 2-ml NHS-activated sepharose (GE Healthcare) and anti-ADF-1 was purified from 45 ml of 1:3 diluted anti-ADF-1 serum (in PBS). The column was washed with 20 ml PBS and the antibody was eluted with 100 mM glycine, pH 2.3 into 1/10th volume 2 M Tris–Cl, 1.5 M NaCl, pH 8.0.

Chromatin crosslinking and chromatin extract preparation of embryos was performed as described at FlyChIP (www.flychip.org) but scaled down 5-fold.

Crosslink and homogenization of 250-mg adult tissue was carried out as described in Nègre *et al.* (39). Samples were centrifuged and rehomogenized twice, coarse matter was sedimented from homogenates by centrifugation at 400g for 1 min at 4°C and supernatants were centrifuged at 1100g for 10 min at 4°C. Pellets were resuspended in 5 ml cell lysis buffer (5 mM PIPES, pH 8.0, 85 mM KCl, 0.5% NP-40, protease inhibitors). The sonication and lysis steps were identical to the FlyChIP protocol.

Immunoprecipitations (IPs) were carried out as described by Perez-Lluch *et al.* (40) with 100 µl of chromatin extract, 1 µg of anti- ADF-1 polyclonal antibody or 1 µg unspecific rabbit immunoglobuline G (IgG) (Sigma). Immunoprecipitated and input DNA (sample prior to IP) was quantified by quantitative PCR with Power SYBR® Green PCR Master Mix (Applied Biosystems) and oligonucleotides (Supplementary Table S1) in an ABI PRISM 7700® Sequence Detection System by absolute standard curve quantifications (41) with serial 4-fold dilutions of specific plasmid DNA (Supplementary Figure S1) and three amplification replicas of each sample.

In vitro transcription

Embryonic nuclear extracts and *in vitro* transcription experiments were performed according to Kamakaka and Kadonaga (42). The preparation of embryonic extracts was scaled down 10-fold with an approximate yield of

1.8 ml of soluble nuclear fraction from 10 g dechorionized *Drosophila* embryos.

Plasmid clones were prepared by standard cloning techniques and contained the *Adh* genes of *D. funebris* and *D. melanogaster* used as the internal control. Plasmids with partial deletions of the *D. funebris Adh* promoter region were prepared by PCR cloning using specific oligonucleotides (Supplementary Table S1). Plasmid DNA was prepared with Miniprep columns, linearized with BamHI (GE-Healthcare) in order to unlink the two *Adh* loci and DNA was quantified with a micro-volume spectrophotometer (Nanodrop).

Data collection and analysis

Sequencing and non-denaturating gels were exposed to imaging screens (Fuji) and the screens were scanned with a TyphoonTM 9400 (GE-Healthcare). Band intensities from EMSA, primer extension products, methylation interference and DNase I footprints were determined with the Quantity One software (BioRad) from non-saturated scans of the entire gel using the level option to maximize visualization of band intensity differences.

Statistical analysis was carried out with the Statgraphics Centurion XVI software.

RESULTS

ADF-1 binding to the predicted binding sites at the *Adh* promoter regions of *D. funebris* and *D. virilis*

Putative ADF-1 binding sites were previously identified in species of the genus *Drosophila* (32,43,44). However, the sequence divergence relative to the ADF-1 binding site of *D. melanogaster* was quite high and we were wondering how those changes at the nucleotide level could potentially translate into differential ADF-1 binding and *Adh* transcriptional regulation. The ADF-1 binding was preliminarily tested *in vitro* for *D. funebris* and *D. virilis* using EMSAs (Figure 1B) with the ADF-1 protein of the species *Scaptodrosophila lebanonensis*. This species is an outgroup to the genus *Drosophila* (45,46). The ADF-1 protein is highly conserved among Drosophilidae species (Lang, M. *et al.*, manuscript in preparation). The 100 amino acids of the N-terminus that contains the DNA binding domain (47) shows 99% of identity between *D. melanogaster* and *S. lebanonensis* and 98% between *S. lebanonensis* and *D. funebris*. The strongest binding was observed for the fragment of *D. funebris*. This fragment includes the two predicted ADF-1 binding sites (32) and as a consequence it is expanded compared with other species. Moderate binding was observed with the *D. virilis* proximal promoter region. No specific ADF-1 binding was observed at the *D. virilis* distal promoter region, in accordance with the previous predictions (43).

In vitro and *in vivo* binding of ADF-1 at the *Adh* promoter of *D. funebris*

The strong binding of ADF-1 observed in the *D. funebris Adh* promoter region was interpreted as the result of binding at the two distinct predicted sites (32). DNase I footprinting was carried out with the ADF-1 protein of *D. funebris*. A large ADF-1 protected region of ~100 bp was detected between positions −97 to −196 relative to the *Adh* transcriptional start site (Figure 2). At low amounts of ADF-1, three subregions were protected that were interspersed with hypersensitive sites (Figure 2). Increasing amounts of ADF-1 progressively expanded the protected regions so that they merged. In comparison, ADF-1 protects a region 40-bp upstream of the *Adh* distal promoter in *D. melanogaster*. (27,33). Our result reveals that the ADF-1 footprint is expanded at the *D. funebris Adh* promoter and that this is one of the explanations for the stronger binding observed in EMSA.

Next, we tested if ADF-1 binds at the *D. funebris Adh* promoter *in vivo* by Chromatin IP (ChIP). ChIPs were performed with chromatin extracts prepared from embryos or 4-day adult flies and with the purified anti-ADF-1 antibody. *In vivo* binding was verified by the enrichment of immunoprecipitated ADF-1 binding regions with respect to control experiments carried out with unspecific IgG (Figure 3). As ADF-1 binding at the *D. melanogaster Adh* distal promoter has been intensely studied *in vitro* (27,30), we performed ChIP experiments with this known interaction as a positive control. Immunoprecipitated DNA and DNA in the chromatin extracts (input sample) were determined by quantitative PCR using the absolute quantification method (41).

A 35–75-fold enrichment of ADF-1 binding regions was detected compared with the control experiments with unspecific IgG carried out in parallel (Figure 3B). The fraction of immunoprecipitated *D. funebris* ADF-1 binding regions with respect to the amounts in each chromatin extracts (input sample) was 0.74% in adult females, 0.9% in adult males and 0.03% in embryos. Comparing those fractions between IPs carried out with anti-ADF-1 or with unspecific IgG revealed highly significant enrichments of anti-ADF-1 immunoprecipitated DNA for embryo, adult female and adult male (Wilcoxon rank sum tests: $P < 0.00042$ each). The total fractions of immunoprecipitated DNA were at similar orders of magnitude compared with experiments with the *D. melanogaster Adh* distal promoter; although stage- and sex-specific differences were observed. The fractions observed with embryonic extracts were always much smaller (Figure 3C). This was probably due to the much higher cell content of embryonic tissues and more genomic DNA in chromatin extracts. Overall, the results confirmed that ADF-1 interacts with the *D. funebris Adh* promoter *in vivo*.

Nucleotide-specific contacts involved in sequence recognition by ADF-1

Methylation interference assays were carried out with *D. funebris* ADF-1 protein in order to determine the guanine nucleotides that contact with ADF-1 in the major groove. However, only a slight interference was observed in the coding strand at positions −163 and −177 (Supplementary Figure S2-1) when we used a DNA fragment with the whole DNase I footprinted

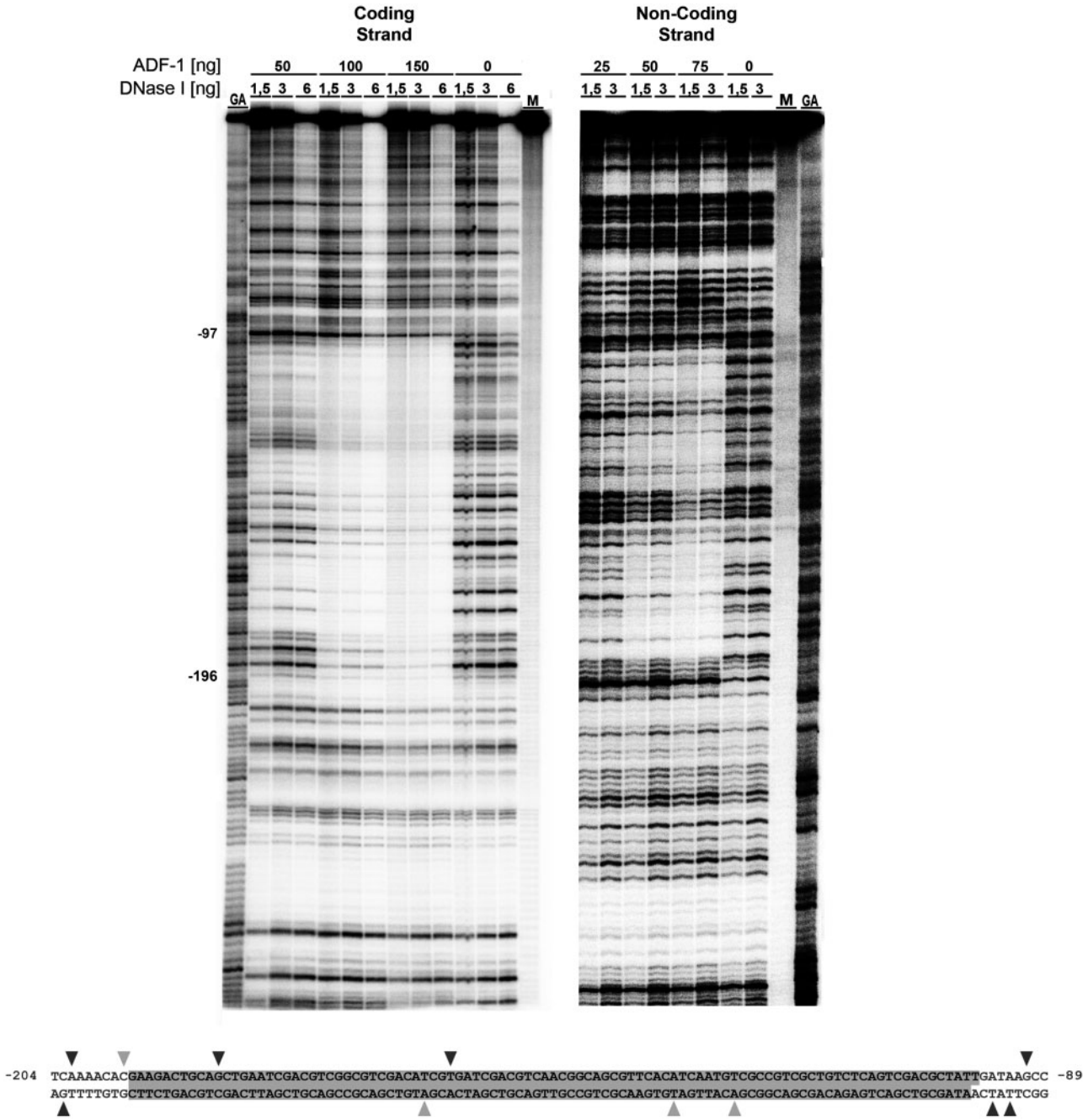

Figure 2. DNase I protection of the ADF-1 Binding region at the *D. funebris Adh* promoter. This experiment was performed with the ADF-1 protein of *D. funebris*. M: Mock experiment, GA: Maxam Gilbert G+A sequencing ladder. Hypersensitive sites are indicated by black triangles, weak hypersensitivity in gray (<150% at 50 ng ADF-1 and 3 ng DNase I).

region. ADF-1 binding at those positions, however, could not account for the large DNase I protected region of ~100 bp. One possible interpretation for this result was the presence of multiple adjacent ADF-1 binding sites within the DNase I protected region. In the methylation interference procedure, EMSA is used to selectively enrich for unmethylated binding sites. In the ideal case of a single binding site per DNA molecule, the bound fraction should get depleted of binding sites with a methylated guanine because it would interfere with the binding of the protein. However, in case of multiple binding sites ADF-1 can bind to unmethylated sites of DNA molecules that carry methylations at adjacent sites. This would prevent the selective enrichment of one particular unmethylated site.

We tested this interpretation by methylation interference assays using PCR products amplified from plasmid clones with partial deletions of the ADF-1 binding region (Figure 4A). In EMSA experiments, the complete deletion of the ADF-1 binding region (p97M) abolished the binding of ADF-1 (Supplementary Figure S3) and longer subregions (p125M, p154M) favored the formation

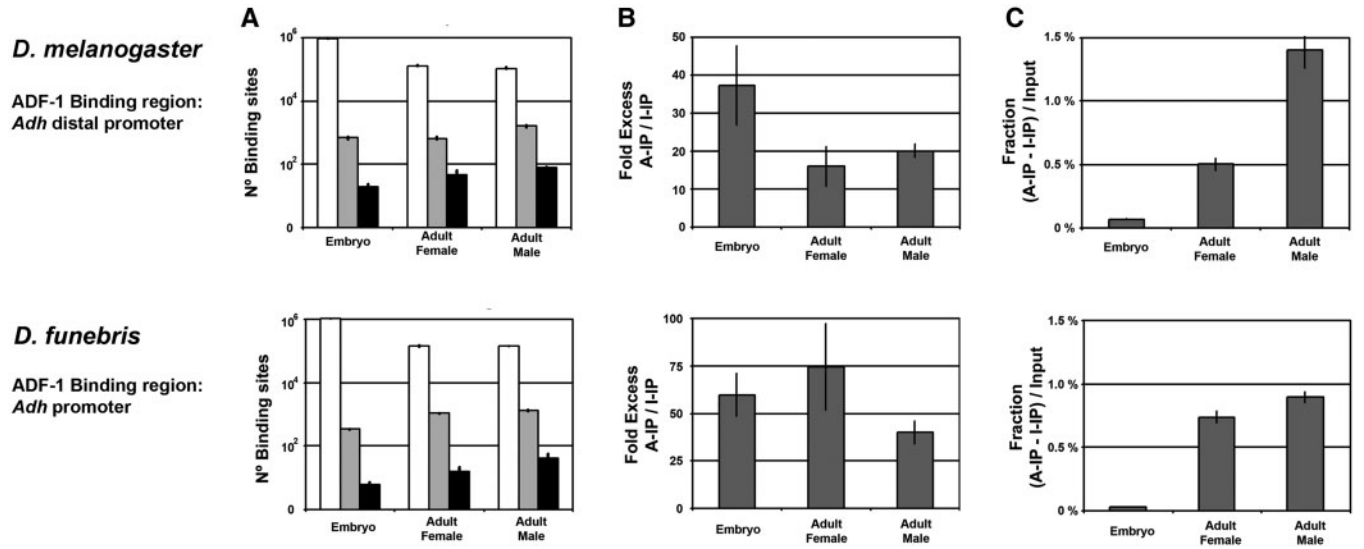

Figure 3. *In vivo* binding of ADF-1 at the *D. funebris Adh* promoter region. (**A**) Quantification of ADF-1 binding sites. The input sample is indicated in white, the anti-ADF-1 ChIP in gray and the control ChIP in black. (**B**) Enrichment of ADF-1 binding sites in anti-ADF-1 ChIP relative to the control IgG ChIP experiments. (**C**) The total fraction of specifically immunoprecipitated DNA with respect to the input sample. A-IP, anti-ADF-1 ChIP; I-IP, control ChIP experiment with unspecific IgG.

of supershifts. In the methylation interference assays, the partial ADF-1 binding region of clone p126M was the smallest and revealed strongest depletion of cleavage fragments between positions −101 to −110 relative to the *Adh* transcriptional start site. The complete region (p5-P) resulted in low discrimination of methylation interference at positions −163 to −177, similar to what had been observed initially (Supplementary Figure S2-1). However, the combination of these different experiments enabled us to identify two elements at the 5′ and 3′ extremes of the ADF-1 binding region that showed the highest interference (Figure 4B). Interestingly, the guanine residues within the subregion of clone p126M that matched the previously published ADF-1 binding consensus (33) did only reveal weak contacts with ADF-1. A methylation interference experiment with this clone and purified *D. melanogaster* ADF-1 was repeated and produced similar results (Supplementary Figure S2-2B).

To test whether the established binding consensus represents well ADF-1 binding preferences, we determined the ADF-1 binding sites within the DNase I protected region at the *D. melanogaster Adh* distal promoter since the results of a previous MPE·FE(II) footprinting (33) lacked of sufficient resolution for a clear determination of the interacting nucleotides. Therefore, we carried out methylation interference experiments with purified *D. melanogaster* ADF-1 and the corresponding promoter region (Supplementary Figure S2-3). ADF-1 interacts much more strongly with the 3′ half of the DNase I protected region although the 5′ half contains the ADF-1 binding consensus established by England *et al.* (33).

Altogether, these results demonstrate that the previously established ADF-1 binding consensus does not represent well the ADF-1 binding preferences although it appears to be conserved among species.

Binding affinity of ADF-1

We further wanted to compare the binding affinities of ADF-1 to the different subregions. EMSA experiments were carried out with double-stranded oligonucleotides of partial sequences of the ADF-1 binding region (Figure 5A).

Oligo 3 contained the subregion with the England's ADF-1 binding consensus. Oligos 1 and 4 contained subregions with most abundant methylation interference sites and Oligo 5 overlapped Oligos 3 and 4. EMSA experiments with these set of oligonucleotides and the protein of *D. funebris* (Figure 5B) or *D. melanogaster* (Supplementary Figure S4) were carried out in three replicates for each oligonucleotide and protein concentration. The low amounts of labeled oligonucleotide (2 ftmol) far below the apparent K_d allowed direct comparisons of the different EMSA experiments performed with each end-labeled oligonucleotide. The apparent dissociation constants (K_d) were estimated for each oligonucleotide (Table 1).

The binding affinities differed among oligonucleotides (Kruskal–Wallis test, *D. funebris* ADF-1: 9.43, $P = 0.024$; *D. melanogaster* ADF-1: 10.3846, $P = 0.016$). The lowest binding affinity of ADF-1 was observed with Oligo 3 that contains the England's consensus. The highest affinity was observed either with Oligo 1 or 4 that contain most of the methylation interference sites. A supershift was observed in experiments with Oligo 5. Since Oligos 3 and 4 only contain one of the two sites, the supershift with Oligo 5 indicates that ADF-1 can simultaneously bind at the two sites. The binding affinites of *D. funebris* and *D. melanogaster* ADF-1 for the oligonucleotides tested were extremely similar with the exception of Oligo 2. However, no significant differences could be detected for any of the four oligonucleotides (*t*-test comparisons, Table 1).

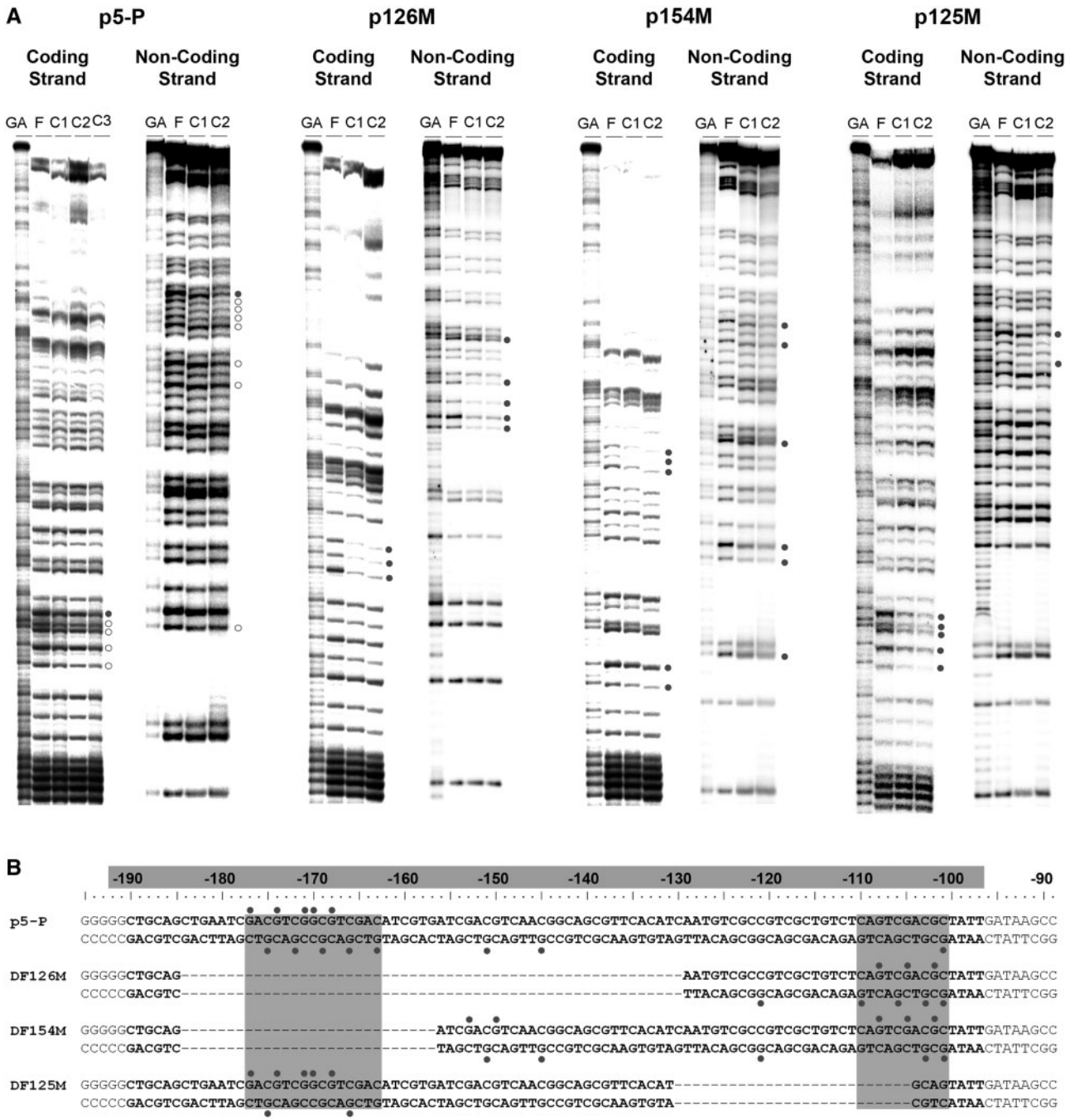

Figure 4. ADF-1 contacts to two subregions of the DNaseI footprint at the *D. funebris Adh* promoter. (**A**) Methylation interference with *D. funebris* ADF-1 and the partial deletion constructs, closed circles indicate guanine residues that interfere with ADF-1 binding when methylated, weak interference sites are indicated by open circles. F: sequencing ladder from unbound DNA, C1, C2 and C3: sequencing ladder from bound DNA, the numbers indicate the order of supershifts. (**B**) ADF-1 DNase I footprint is indicated by the gray bar, subregions with abundant methylation interference sites are shaded gray.

We also wanted to compare the ADF-1 binding region of *D. funebris* with the shorter orthologous region of *D. virilis*. Although the *D. virilis* ADF-1 binding region has not been characterized by DNase I footprinting, it could be deduced from DNA sequence comparisons using our data. The *D. funebris* ADF-1 binding region in the plasmid p5 was replaced by a 41-bp double-stranded oligonucleotide (DFDV) that contained the putative binding region of *D. virilis* (Supplementary Figure S2-4A). The cloned *D. virilis* ADF-1 binding region was amplified by PCR and characterized by EMSA and methylation interference assays (Supplementary Figure S2-4). Using *D. funebris* ADF-1, we identified the guanines that when methylated interfere with the binding in a region of 23 bp. This region was much shorter than the complex ADF-1 binding region of the *D. funebris Adh* promoter. The ADF-1 binding region of *D. funebris* (p5-P) was also amplified and

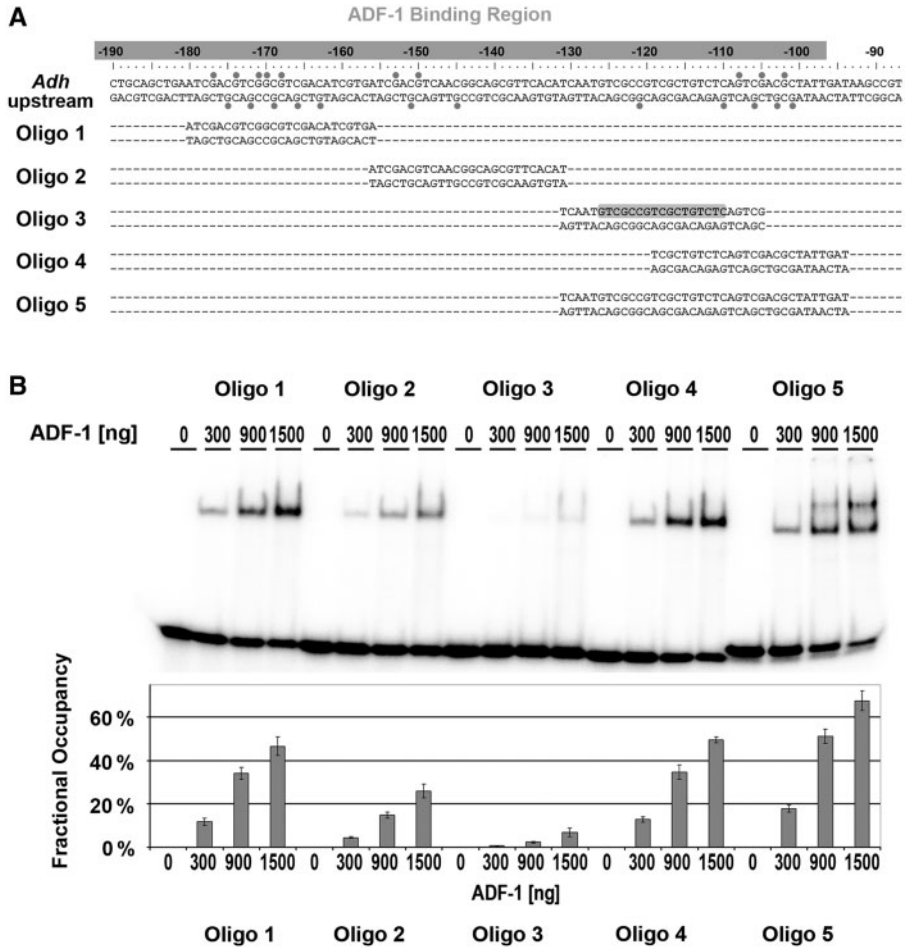

Figure 5. ADF-1 binding affinity for the different elements in the binding region. (**A**) Double-stranded oligonucleotides. The ADF-1 footprint is indicated by a gray bar. Methylation interference sites are indicated by gray closed circles and the sequence that follows the England's ADF-1 binding consensus is highlighted in the forward strand of Oligo 3. (**B**) Comparison of ADF-1 binding affinity to the Oligonucleotides 1–5. Representative EMSA's are shown with *D. funebris* ADF-1.

Table 1. Apparent K_d estimates for ADF-1 and specific oligos

Template	*Drosophila funebris*		*Drosophila melanogaster*		*t*-test	*F*-test
	Apparent K_d [M]	standard deviation (SD)	Apparent K_d [M]	standard deviation (SD)	*P*-value	*P*-value
Oligo 1	1.95E-06	±2.54E-07	1.98E-06	±2.25E-07	0.888	0.878
Oligo 2	5.05E-06	±2.41E-07	4.07E-06	±6.89E-07	0.083	0.217
Oligo 3	2.83E-05	±7.97E-06	2.75E-05	±9.25E-06	0.913	0.852
Oligo 4	1.86E-06	±1.77E-07	1.63E-06	±8.85E-08	0.120	0.400

Binding affinities were approximated by least square fits of a one site binding model (52) to the experimental data. The *t*-test of comparisons between the binding affinities obtained with *D. funebris* and *D. melanogaster* ADF-1 show no significant differences (95% confidence interval (CI), *t*-values for Oligos 1, −2, −3, and −4: −0.15043, 2.30268, 0.11591 and 1.97116, respectively). The *F*-test indicates no significant differences of standard deviations (SD) of the compared samples (*F*-values for Oligos 1, −2, −3, −4: 1.27854, 0.121707, 0.742883, and 4.00484, respectively).

analyzed by EMSA with ADF-1 of this species in order to compare ADF-1 binding with both regions (Figure 6A). Furthermore, ADF-1 binding to the double-stranded oligonucleotide DFDV was compared with the binding to Oligos 1 and 5 (Figure 6B). The ADF-1 quantities required for 50% fractional occupancy (Supplementary Table S2) were determined by regression in order to compare overall binding of ADF-1 to the different binding targets. This simple analysis was preferred to a binding model fit to the data because of the different numbers of binding sites present in each tested binding region.

Comparisons of the entire binding regions revealed stronger binding of ADF-1 to the larger *D. funebris* binding region (*t*-test: $t = 16.834$, $P < 0.00008$; *F*-test for similar standard deviations: $F = 0.08858$, $P = 0.16274$).

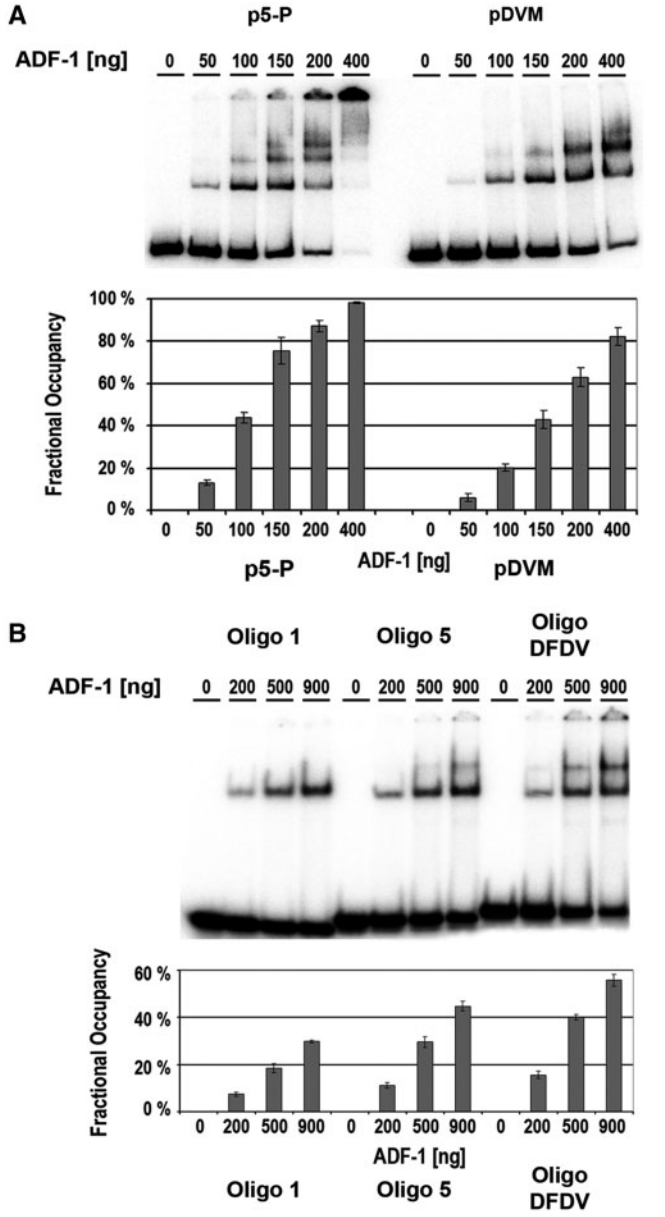

Figure 6. Comparison of ADF-1 binding affinity to the *D. virilis Adh* proximal promoter and *D. funebris* promoter. (**A**) Binding of ADF-1 of *D. funebris* to the entire binding regions of *D. funebris* and *D. virilis*. (**B**) Binding of ADF-1 to the double-stranded oligonucleotides DFDV, Oligos 1 and 5.

On the contrary, we observed a 10% higher fractional occupancy of the *D. virilis* oligonucleotide DFDV compared with those of Oligos 1 and 5 (multiple range test: three significantly distinct groups). This result shows that the increased overall binding of ADF-1 to the *D. funebris* promoter region is the consequence of the regional expansion of the ADF-1 binding region and it is not due to higher binding affinities at specific ADF-1 binding sites.

High-affinity binding site consensus for ADF-1

The DNA binding experiments with ADF-1 to the *Adh* regulatory promoter of different Drosophilidae species demonstrate that the England's ADF-1 binding consensus $[G^C/_T C/_T]_{4-5}$ does not match ADF-1 binding preferences. Also, previous work with the *Adh* distal promoter already supported that ADF-1 binds with highest affinity to sites that do not follow England's consensus (27).

The binding site preferences and affinities resulted to be extremely similar for the different orthologous ADF-1 proteins of *D. melanogaster*, *D. funebris* and *S. lebanonensis* (Supplementary Figures S2-2, S2-5 and S6). This prompted us to combine the results of the reported methylation interference experiments and to determine an ADF-1 binding consensus sequence that better describes the sequence motifs with high ADF-1 binding affinity. Most of the binding sites with high ADF-1 binding affinities contained the motif $[G^T/_C CG^G/_A C]$ (Figure 7A). These sequences were aligned to establish the high-affinity consensus (Figure 7B). The sites Dmel 1, Dfun 2 and Dvir 1 were excluded from the comparison because those either contain only a few methylation interference sites and/or have lower affinity values. The obtained sequence logo with the core sequence of 9 bp $G^T/_C C/_T G^G/_A CG^T/_C C/_T$ differs from England's consensus by being 3 bp shorter. Furthermore, it differs at the positions 5 and 6 with $^G/_A$ and *C*, respectively, instead of $^C/_T C/_T$. These differences apparently account for the difference between high and low ADF-1 binding affinties.

Functional contribution of the different binding sites to *Adh* transcription

The transcriptional activity of ADF-1 binding sites in the *Adh* regulatory promoter of *D. funebris* and *D. virilis* was tested by *in vitro* transcription using embryonic nuclear extracts of *D. melanogaster*.

The DNA templates for *in vitro* transcription were the plasmid clones with a mutated *D. funebris Adh* regulatory promoter (Figure 4B) and the *D. melanogaster Adh* distal promoter as the internal control (Supplementary Figure S2). The transcription of the *D. funebris Adh* gene was first tested in the presence or absence of the ADF-1 binding region or the *TGATAA* element (Figure 8A).

The band intensities of primer extension products of each *in vitro* transcribed *D. funebris Adh* template were compared with the *in vitro* transcription of the *D. melanogaster Adh* distal promoter template used as internal control. We first compared the amount of *D. melanogaster Adh* distal transcript obtained from each clone in order to verify independent transcription from the different promoters within each experiment. Transcription with clone p7 which contains only the *Adh* gene of *D. melanogaster* was similar to that of clones p5-PS, p5-PGM and p97S that additionally contained the *D. funebris Adh* insert (Figure 8A). Decreased transcription levels of clone p97GM were due to erroneous plasmid quantifications.

Removal of either the *TGATAA* element (p5-PGM) or the ADF-1 binding region (p97S) or both (p97GM) resulted in a progressive decrease of *D. funebris Adh* transcription from 92.5% to 59% relative to clone p5-PS (analysis of variance (ANOVA): $F = 246.34$, $P < 0.00001$; Figure 8B). A reduction of 25% of *D. funebris Adh*

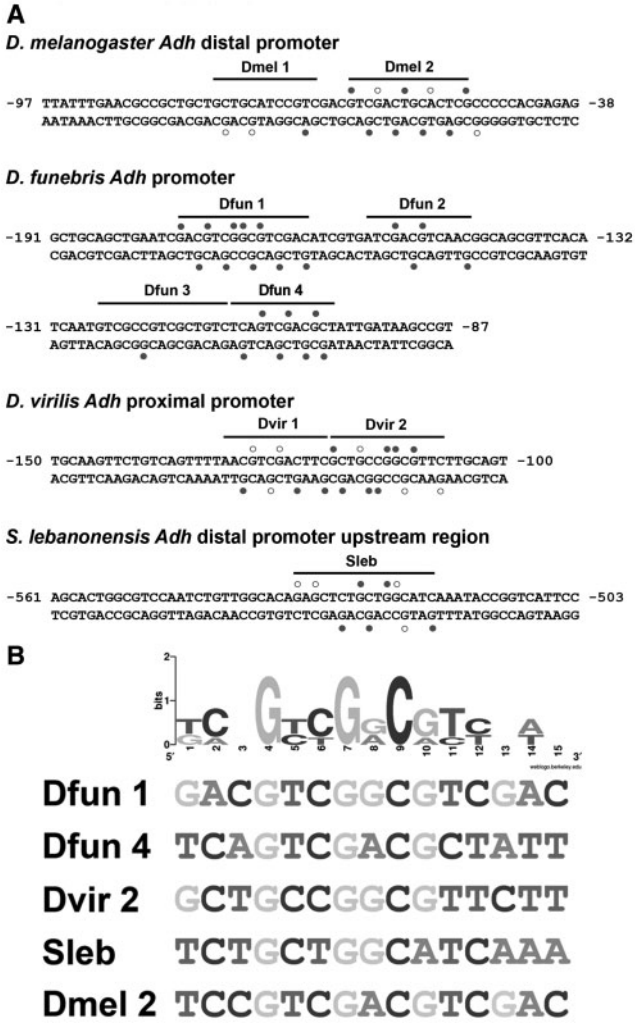

Figure 7. ADF-1 binding sites upstream of the *Adh* gene in Drosophilidae and ADF-1 high-affinity binding consensus. (**A**) ADF-1 binding sites are recognized as regions of maximal 17 bp that contain at least three nearby methylation interference sites. The site Dfun 3, which contains the England's consensus, shows the lowest binding affinity by ADF-1 as determined by the binding to Oligos 5 and 3. The closed circles indicate strong methylation interference while open circles indicate partial methylation interference. Sequence positions indicate the distances to the transcriptional start site. (**B**) The sequence logo was established with Weblogo (www.weblogo.berkely .edu).

transcription was observed with removal of the ADF-1 binding region. This value was three times higher than that observed with the lack of the *TGATAA* element, which caused a reduction of 8% only.

Finally, the partial deletions of the ADF-1 binding region of the clones p126GM, p154GM, p125GM and pDVGM with the mutated *TGATAA* element were tested for differential *D. funebris Adh* transcription (Figure 8C). Decreased *D. funebris Adh* transcription was observed with all deletion clones compared with clone p5-PGM (ANOVA: $F = 135.921$, $P < 0.00001$). Using a multiple range test, we determined five distinct homogenous groups of the six different experiments with similar expression levels detected for clones p154GM and pDVGM. A maximal reduction of 36% was obtained with clone p97GM relative to clone p5-PGM (Figure 8D).

The magnitude of expression differences was comparable with the results of previous *in vitro* transcription studies with the *Adh* proximal promoter of *D. melanogaster* and *D. affinidisjuncta* (27,48). An advantage to the previous studies was the use of the *D. melanogaster Adh* distal promoter transcription as internal control experiment. This enabled us to discriminate between small expression differences because of the robustness to the experimental error. A reduction of 8% of transcription was observed with clone p125GM that contained a deletion of the 3′ ADF-1 binding region. For the complementary deletion of clone p126GM, a 20% reduction of transcription was observed.

Clones p154GM and pDVGM showed 13% reduction of transcription. Thus, the *D. virilis* ADF-1 binding region in the context of the *D. funebris Adh* promoter partially rescues the loss of *D. funebris* ADF-1 binding region.

The clones p154GM and p125GM contained binding regions of equal length, but lacked either the 5′or the 3′ region for which ADF-1 shows the highest affinity. The *Adh* transcription with clone p125GM was 5% higher, thus the 5′ ADF-1 binding region enhanced *Adh* transcription more efficiently. Overall, regional extensions of the ADF-1 binding region as well as sequence-specific effects seem to enhance *Adh* transcription in an additive manner.

DISCUSSION

Length and composition of the ADF-1 binding region

ADF-1 binds with different affinities to at least four DNA binding sites within a region of ~100-bp upstream of the *D. funebris Adh* promoter. Our data imply that at low concentrations, ADF-1 binds to the most affine sites and increasing concentrations successively lead to the coverage of the entire binding region. The ADF-1 binding sites with the highest binding affinities are located at the 5′ and at the 3′-end of this region. The orthologous binding region at the *Adh* proximal promoter of *D. virilis* is shorter and consists of two adjacent sites Dvir1 and Dvir2 that give rise to two mobility shift complexes in EMSA experiments. This shows that one of the mechanisms of diversification of ADF-1 binding regions is the gain and loss of entire recognition sites. Multiple adjacent binding sites were also reported for other transcription factors in *Drosophila*, such as *bcd*, *Ubx* or *Zeste* (49–51).

One aspect in the variation of binding region expansion is the probable response to different ADF-1 cellular concentrations. The more sites are encountered in the binding region, the higher is the probability that at least one of them is bound by ADF-1. This is observed *in vitro* when we compare the ADF-1 binding regions of *D. funebris* and *D. virilis*. *D. virilis* contains two ADF-1 recognition sites in the region. However, the EMSA experiments show a higher fractional occupancy of the ADF-1 binding region of *D. funebris* which does not contain binding sites with higher affinity than those of *D. virilis* but with more binding sites. In this case, it is the gain of sites that increases ADF-1 binding. Altogether, the extension of

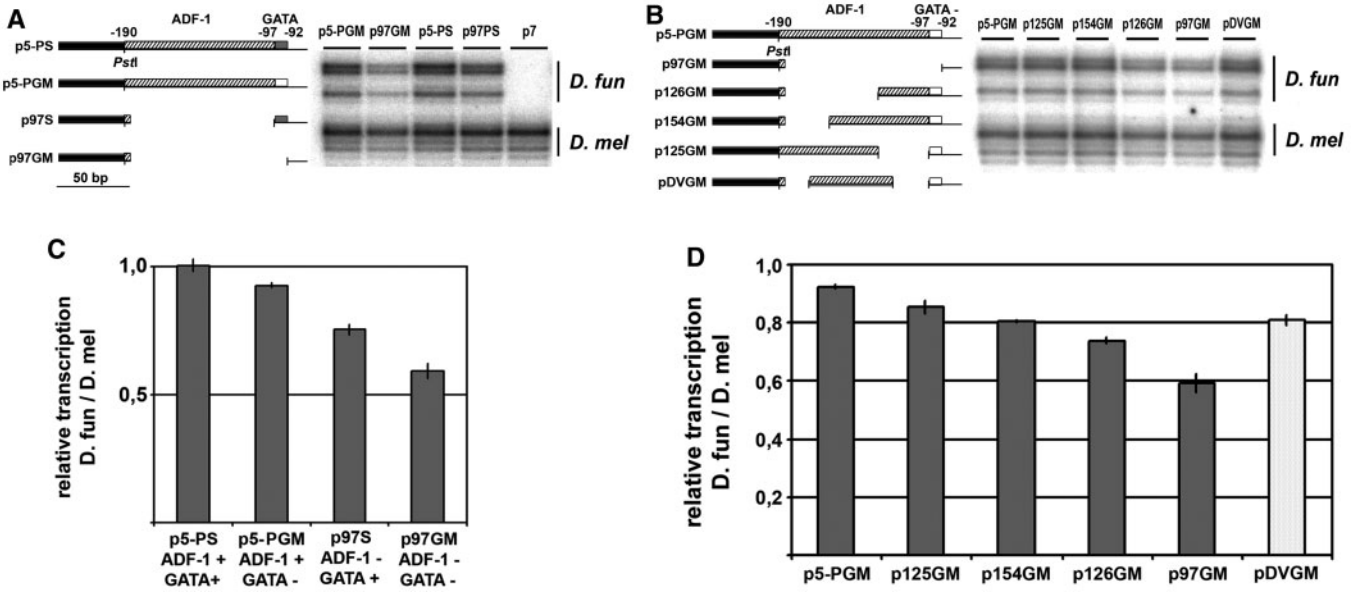

Figure 8. *In vitro* transcription of *D. funebris Adh* deletion constructs. (**A**) Deletion mutation constructs, the intact GATA element is indicated by the gray box and the mutated element by the white box; the ADF-1 binding region is marked with the dashed boxes. Primer extension bands are labeled *D. fun*, *D. funebris* transcripts; *D. mel*, *D. melanogaster* transcripts. (**B**) Quantification of primer extension band intensities. Four distinct homogenous groups identified by multiple range test (95% CI). (**C**) Partial deletion constructs of the ADF-1 binding region at the *D. funebris Adh* promoter. (**D**) Quantification of primer extension band intensities. Five distinct homogenous groups identified by multiple range test (95% CI), joining pDVGM and p154GM.

ADF-1 binding regions could potentially compensate for lower ADF-1 expression levels *in vivo*.

ADF-1 high-affinity consensus

The EMSA experiments with double-stranded oligonucleotides, demonstrate that the binding site Dfun 3 ($[G^C/_T C^C/_T]_4$), which matches the England's binding consensus is a weak binding site. Isolated from the regional context in Oligo 3, we observed a >10-fold reduced affinity of ADF-1 to this site compared with its affinity for the sites Dfun 1 and Dfun 4. However, this site appears to be functional in the presence of the adjacent site Dfun 4 within Oligo 5, detectable by the formation of the supershifts at protein concentrations equal or higher than 1.003 μM. This observation prompted us to consider that ADF-1 binding to the site Dfun 3 might require cooperative interactions with ADF-1 bound at the adjacent site Dfun 4.

Cooperative interactions can be evaluated with titrations of transcription factor concentrations in series of EMSA experiments (52). Using this approach, cooperative binding was determined for a number of transcription factors such as *LacI*, CAP, *Ubx bicoid* or λ-repressor (49,52–54). Although we have not performed such a fine analysis of ADF-1 binding kinetics, we used our experimental data to fit the constants to a simple two binding site model, following Senear and Brenowitz (52) (Supplementary Figure S6 and Table S3). The fit of the model to our experimentally determined fractional occupancies strongly indicated cooperative interactions between ADF-1 proteins bound to the two adjacent sites Dfun 3 and Dfun 4 (Supplementary Table S3). Similar results were obtained for the transcription factor *Ubx* that was found to bind to clusters of multiple individual binding site sequences downstream of its own promoter and close to the transcriptional start site of the Antp P1 promoter (55). Interactions at the Ubx locus with other distant UBX DNA complexes further leads to the formation of DNA loops (49). UBX binding interactions are cooperative and the multiple binding sites have different binding affinities. Cooperative binding was also reported for the *Adf-1* structural homolog *Zeste* (50). The ability to form cooperative interactions could probably be mediated by the C-terminus of ADF-1. This functional domain was also responsible for other protein–protein interactions, such as the formation of homodimers and the protein–protein contacts with TAF 110 and TAF 250 (47).

Assuming cooperative interactions between ADF-1 molecules that bind at adjacent or near binding sites, the functional conservation of low-affinity sites would therefore not require high sequence conservation. However, during evolution the high-affinity site should remain conserved, while adjacent sites could accumulate changes to some extent. In addition, new binding sites could evolve with few changes in proximity to the high-affinity sites. This molecular mechanism would further explain the origin of the different expansions of the two analyzed orthologous ADF-1 binding regions of *D. funebris* and *D. virilis*.

We have demonstrated with different experiments that the England's binding consensus for ADF-1 is not fully compatible with high-affinity binding sites but is fully compatible with low-affinity sites. The analysis of ADF-1 binding regions at other *D. melanogaster* gene promoters, as *Adh* proximal, *Ddc* and *Antp P1*, (33) encountered several motifs within ADF-1 DNase I protected regions that follow well this low-affinity consensus

(Supplementary Figure S5A). However, the footprints were obtained with 5 to 10 times more protein than for the distal *Adh* promoter that has the high-affinity consensus. Also the protected region in the *dpp* gene obtained with nuclear extracts showed the low-affinity consensus (56). The re-examination of the ADF-1 binding regions of those genes revealed the lack of high-affinity binding sites (Supplementary Figure S5A). This shows that the motif described by England *et al.* (33) is an abundant sequence within ADF-1 binding regions and it is obviously the reason why it was proposed as the binding consensus although previous data did not support this interpretation. Footprinting experiments with partial deletions of the *D. melanogaster Adh* distal promoter showed that the important portion for binding did not contain England's consensus (27). The re-examination of the deleted sequence that reduced 70% of DNase I protection has revealed that it has the high-affinity consensus, described in this study. The presence of both, high- and low-affinity recognition sites within ADF-1 binding regions may constitute structural features that act as complex binding targets.

We have also shown that the binding site preferences are conserved among the different ADF-1 orthologus proteins of *D. melanogaster*, *D. funebris* and *S. lebanonensis* (Figure 4, Supplementary Figures S2-2 and S2-5) as expected from the high amino acid sequence conservation in the DNA binding domain.

Adh transcription mediated by the ADF-1 binding region

The experimental design of the *in vitro* transcription experiments allowed us to detect minor changes of transcriptional activity based on the use of an internal control in the same plasmid that reduced the experimental error. The ADF-1 binding region enhances *Adh* transcription as well as a conserved transcription factor binding site for the *Drosophila* GATA homolog ABF-1 that was shown to be a functional element at the orthologous promoters of *D. melanogaster*, *D. mulleri* (57) and *D. affinidisjuncta* (48). ABF-1 is expressed in the embryonic fat body (57) and was shown to be present in embryonic nuclear extracts of *D. melanogaster* (48). Thus, we assume that ABF-1 also binds to this site in *D. funebris* and activates *Adh* transcription, as demonstrated for the other species.

The enhancement of *Adh* transcription by ADF-1 and ABF-1 is probably additive but not synergic. Synergic effects are observed among factors that bind close to the transcriptional start site by simultaneous interactions with different parts of the transcriptional machinery (58,59). The moderately accumulative activation of *Adh* transcription in response to those elements suggests that in *D. funebris* ABF-1 and ADF-1 enhance *Adh* transcription independently and are involved in different molecular mechanisms.

Removal of the GATA element in the presence of the ADF-1 binding region caused a reduction of 8% of the *Adh* transcription. Similarly, removal of the ADF-1 binding region reduced 25% *Adh* transcription in the presence of the GATA element and 41% in its absence instead of the 33% expected if it was strictly additive. This shows that the effect of the deletion of one element on *Adh* transcription is greater in the absence of another and that one element could partially compensate for the absence of the other. The ADF-1 binding region at the *Adh* proximal promoter of *D. melanogaster* is less expanded than in *D. funebris* and does not have any high-affinity binding site. According to previous data, this region did not appear to be critical for *Adh* transcription (27). Possibly, this smaller ADF-1 binding region is embedded in between other activating elements. Those might enhance transcription and could have compensated the loss of ADF-1 mediated *Adh* transcriptional activation similar to what we observed in our experiments with the *D. funebris Adh* promoter.

The orthologous ADF-1 binding region of *D. virilis* in the context of the *D. funebris Adh* promoter enhances *Adh* transcription, but 13% less efficiently than the endogenous *D. funebris* ADF-1 binding region. This suggests that the expansion of the ADF-1 binding region in *D. funebris* has increased the effect of ADF-1 on *Adh* transcription. However, the absolute difference in *Adh* transcriptional activation is quite small. Therefore, the probable biological function of this expanded region might be better interpreted as an adaptation to compensate for lower absolute expression levels of ADF-1 in certain tissues rather than enhancing *Adh* transcription. Similar findings were discussed for other transcription factors, such as *BCD* (35). Clusters of high- and low-affinity binding sites were evaluated *in silico* in known regulatory regions and it was concluded that the composition of such site clusters scattered over genomic regions of ~500 bp potentially mediates differential transcriptional responses to a given transcription factor concentration. A stochastic enrichment of binding interactions does occur *in vitro* at the characterized ADF-1 binding region as revealed by EMSA (Figure 6B).

Overall, the expanded ADF-1 binding region exemplifies the structural change of the *Adh* promoter region in *D. funebris*. We detected conservation of this expansion in the related species *D. kuntzei* and *D. immigrans*. At least for *D. kuntzei* it is known that the *Adh* gene is also transcribed from a single promoter (44). Molecular phylogenetic analysis of Drosophilidae (46,60) demonstrates that these three species form a monophyletic group within the subgenus Drosophila. The expansion of the ADF-1 binding region at the *Adh* proximal promoter in this lineage can further be associated with the loss of the *Adh* distal promoter, either as compensation or as a predating regulatory change that might have allowed its disappearance.

SUPPLEMENTARY DATA

Supplementary Data are available at NAR Online.

ACKNOWLEDGEMENTS

We thank A. Pérez-Farrerons for his valuable help in the preparation of embryonic nuclear extracts, methylation

interference and *in vitro* transcription experiments. We are grateful to P. Librado for his help and the estabishment of the phastCons conservation scores. We also thank M.L. Espinàs and S. Lluch-Pérez for their helpful comments on ChIP analysis. The radioactive experiments were performed in the Servei de Radioctivitat of the Facultat de Biologia (UB) under the supervision of C. Benito. The real-time PCR and automated sequencing of clones was carried out in the Serveis Cientifc Tècnics (SCT-UB) under the supervision of A. Amador and R. Seminago.

FUNDING

Ministerio de Educación y Ciencia (MEC) (grant BFU 2004-00668 to E.J.); the Comissió Interdepartamental de Recerca I Innovació Tecnològica (CIRIT) (grant 2005SGR 0166 to M. Aguadé); Generalitat de Catalunya [pre-doctoral fellowship (FI-IQUC 2004-2007) to M.L.]. Funding for open access charge: Comissió Interdepartamental de Recerca i Innovació Tecnològica Generalitat de Catalunya.

Conflict of interest statement. None declared.

REFERENCES

1. King,M.-C. and Wilson,A.C. (1975) Evolution at two levels in humans and chimpanzees. *Science*, **188**, 107–116.
2. Carroll,S.B. (2008) Evo-devo and an expanding evolutionary synthesis: a genetic theory of morphological evolution. *Cell*, **134**, 25–36.
3. Prud'homme,B., Gompel,N. and Carroll,S.B. (2007) Emerging principles of regulatory evolution. *Proc. Natl Acad. Sci. USA*, **104**, 8605–8612.
4. Ludwig,M.Z. (2002) Functional evolution of noncoding DNA. *Curr. Opin. Genet. Dev.*, **12**, 634–639.
5. Ludwig,M.Z., Palsson,A., Alekseeva,E., Bergman,C.M., Nathan,J. and Kreitman,M. (2005) Functional Evolution of a cis-Regulatory Module. *PLoS Biol.*, **3**, e93.
6. Bejerano,G., Pheasant,M., Makunin,I., Stephen,S., Kent,W.J., Mattick,J.S. and Haussler,D. (2004) Ultraconserved elements in the human genome. *Science*, **304**, 1321–1325.
7. Plessy,C., Dickmeis,T., Chalmel,F. and Strahle,U. (2005) Enhancer sequence conservation between vertebrates is favoured in developmental regulator genes. *Trends Genet.*, **21**, 207–210.
8. Sandelin,A., Bailey,P., Bruce,S., Engstrom,P., Klos,J., Wasserman,W., Ericson,J. and Lenhard,B. (2004) Arrays of ultraconserved non-coding regions span the loci of key developmental genes in vertebrate genomes. *BMC Genomics*, **5**, 99.
9. Vavouri,T., Walter,K., Gilks,W., Lehner,B. and Elgar,G. (2007) Parallel evolution of conserved non-coding elements that target a common set of developmental regulatory genes from worms to humans. *Genome Biol.*, **8**, R15.
10. Venkatesh,B., Kirkness,E.F., Loh,Y.-H., Halpern,A.L., Lee,A.P., Johnson,J., Dandona,N., Viswanathan,L.D., Tay,A., Venter,J.C. *et al.* (2006) Ancient Noncoding Elements Conserved in the Human Genome. *Science*, **314**, 1892.
11. Woolfe,A., Goodson,M., Goode,D., Snell,P., McEwen,G., Vavouri,T., Smith,S., North,P., Callaway,H. and Kelly,K. (2005) Highly conserved non-coding sequences are associated with vertebrate development. *PLoS Biol.*, **3**, e7.
12. Ludwig,M.Z., Bergman,C., Patel,N.H. and Kreitman,M. (2000) Evidence for stabilizing selection in a eukaryotic enhancer element. *Nature*, **403**, 564–567.
13. Ludwig,M.Z., Patel,N.H. and Kreitman,M. (1998) Functional analysis of eve stripe 2 enhancer evolution in Drosophila: rules governing conservation and change. *Development*, **125**, 949–958.
14. Segal,E., Raveh-Sadka,T., Schroeder,M., Unnerstall,U. and Gaul,U. (2008) Predicting expression patterns from regulatory sequence in Drosophila segmentation. *Nature*, **451**, 535–540.
15. Segal,E. and Widom,J. (2009) From DNA sequence to transcriptional behaviour: a quantitative approach. *Nat. Rev. Genet.*, **10**, 443–456.
16. Badis,G., Berger,M.F., Philippakis,A.A., Talukder,S., Gehrke,A.R., Jaeger,S.A., Chan,E.T., Metzler,G., Vedenko,A., Chen,X. *et al.* (2009) Diversity and complexity in DNA recognition by transcription factors. *Science*, **324**, 1720–1723.
17. Abel,T., Bhatt,R. and Maniatis,T. (1992) A Drosophila CREB/ATF transcriptional activator binds to both fat body- and liver-specific regulatory elements. *Genes Dev*, **6**, 466–480.
18. Ayer,S. and Benyajati,C. (1990) Conserved enhancer and silencer elements responsible for differential Adh transcription in Drosophila cell lines. *Mol. Cell. Biol.*, **10**, 3512–3523.
19. Ayer,S., Walker,N., Mosammaparast,M., Nelson,J.P., Shilo,B.Z. and Benyajati,C. (1993) Activation and repression of Drosophila alcohol dehydrogenase distal transcription by two steroid hormone receptor superfamily members binding to a common response element. *Nucleic Acids Res.*, **21**, 1619–1627.
20. Benyajati,C., Ayer,S., McKeon,J., Ewel,A. and Huang,J. (1987) Roles of cis-acting elements and chromatin structure in Drosophila alcohol dehydrogenase gene expression. *Nucleic Acids Res.*, **15**, 7903–7920.
21. Benyajati,C., Ewel,A., McKeon,J., Chovav,M. and Juan,E. (1992) Characterization and purification of Adh distal promoter factor 2, Adf-2, a cell-specific and promoter-specific repressor in Drosophila. *Nucleic Acids Res.*, **20**, 4481–4489.
22. Corbin,V. and Maniatis,T. (1990) Identification of cis-regulatory elements required for larval expression of the Drosophila melanogaster alcohol dehydrogenase gene. *Genetics*, **124**, 637–646.
23. Corbin,V. and Maniatis,T. (1989) Role of transcriptional interference in the Drosophila melanogaster Adh promoter switch. *Nature*, **337**, 279–282.
24. Corbin,V. and Maniatis,T. (1989) The role of specific enhancer-promoter interactions in the Drosophila Adh promoter switch. *Genes Dev.*, **3**, 2191–2120.
25. Fischer,J.A. and Maniatis,T. (1988) Drosophila Adh: a promoter element expands the tissue specificity of an enhancer. *Cell*, **53**, 451–461.
26. Hansen,S.K. and Tjian,R. (1995) TAFS and TFIIA mediate differential utilization of the tandem Adh promoters. *Cell*, **82**, 565–575.
27. Heberlein,U., England,B. and Tjian,R. (1985) Characterization of Drosophila transcription factors that activate the tandem promoters of the alcohol dehydrogenase gene. *Cell*, **41**, 965–977.
28. Jackson,J.R. and Benyajati,C. (1993) DNA-histone interactions are sufficient to position a single nucleosome juxtaposing Drosophila Adh adult enhancer and distal promoter. *Nucleic Acids Res.*, **21**, 957–967.
29. Ren,B. and Maniatis,T. (1998) Regulation of Drosophila Adh promoter switching by an initiator-targeted repression mechanism. *EMBO J.*, **17**, 1076–1086.
30. Heberlein,U. and Tjian,R. (1988) Temporal pattern of alcohol dehydrogenase gene transcription reproduced by Drosophila stage-specific embryonic extracts. *Nature*, **331**, 410–415.
31. Amador,A. and Juan,E. (1999) Nonfixed duplication containing the Adh gene and a truncated form of the Adhr gene in the Drosophila funebris species group: Different modes of evolution of Adh relative to Adhr in Drosophila. *Mol. Biol. Evol.*, **16**, 1439–1456.
32. Amador,A., Papaceit,M. and Juan,E. (2001) Evolutionary change in the structure of the regulatory region that drives tissue and temporally regulated expression of alcohol dehydrogenase gene in Drosophila funebris. *Insect Mol. Biol.*, **10**, 237–247.
33. England,B.P., Heberlein,U. and Tjian,R. (1990) Purified Drosophila transcription factor,Adh distal factor-1 (Adf-1), binds to sites in several Drosophila promoters and activates transcription. *J. Biol. Chem.*, **265**, 5086–5094.
34. Kim,J., He,X. and Sinha,S. (2009) Evolution of regulatory sequences in 12 *Drosophila* species. *PLoS Genet.*, **5**, e1000330.

35. Lifanov,A.P., Makeev,V.J., Nazina,A.G. and Papatsenko,D.A. (2003) Homotypic Regulatory Clusters in Drosophila. *Genome Res.*, **13**, 579–588.
36. Gaul,U., Seifert,E., Schuh,R. and Jäckle,H. (1987) Analysis of Krüppel protein distribution during early Drosophila development reveals posttranscriptional regulation. *Cell*, **50**, 639–647.
37. Sambrook,J. and Russel,D.W. (2001) *Molecular Cloning, A Laboratory Manual*, 3 edn. Cold Spring Harbor Laboratory Press, Cold Spring Harbor, New York.
38. Carey,M. and Smale,S.T. (2001) *Transcriptional Regulation in Eukaryotes*. Cold Spring Harbor Laboratory Press, New York.
39. Nègre,N., Hennetin,J., Sun,L.V., Lavrov,S., Bellis,M., White,K.P. and Cavalli,G. (2006) Chromosomal Distribution of PcG Proteins during *Drosophila* Development. *PLoS Biol.*, **4**, e170.
40. Perez-Lluch,S., Cuartero,S., Azorin,F. and Espinas,M.L. (2008) Characterization of new regulatory elements within the Drosophila bithorax complex. *Nucleic Acids Res.*, **36**, 6926–6933.
41. Whelan,J.A., Russell,N.B. and Whelan,M.A. (2003) A method for the absolute quantification of cDNA using real-time PCR. *J. Immunol. Methods*, **278**, 261–269.
42. Kamakaka,R.T. and Kadonaga,J.T. (1994) The soluble nuclear fraction, a highly efficient transcription extract from Drosophila embryos. *Methods Cell Biol.*, **44**, 225–235.
43. Nurminsky,D.I., Moriyama,E.N., Lozovskaya,E.R. and Hartl,D.L. (1996) Molecular phylogeny and genome evolution in the Drosophila virilis species group: Duplications of the alcohol dehydrogenase gene. *Mol. Biol. Evol.*, **13**, 132–149.
44. Oppentocht,J.E., van Delden,W. and van de Zande,L. (2002) Isolation and characterization of the genomic region from Drosophila kuntzei containing the Adh and Adhr genes. *Mol. Biol. Evol.*, **19**, 1026–1040.
45. Grimaldi,D.A. (1990) A phylogenetic, revised classification of genera in the Drosophilidae (Diptera). *Bull. Am. Mus. Nat. Hist.*, **197**, 1–139.
46. Russo,C.-A.M., Takezaki,N. and Nei,M. (1995) Molecular phylogeny and divergence times of Drosophilid species. *Mol. Biol. Evol.*, **12**, 391–404.
47. Cutler,G., Perry,K.M. and Tjian,R. (1998) Adf-1 Is a nonmodular transcription factor that contains a TAF-binding Myb-like motif. *Mol. Cell. Biol.*, **18**, 2252–2261.
48. Hu,J., Qazzaz,H. and Brennan,M.D. (1995) A transcriptional role for conserved footprinting sequences within the larval promoter of a Drosophila alcohol dehydrogenase gene. *J. Mol. Biol.*, **249**, 259–269.
49. Beachy,P.A., Varkey,J., Young,K.E., von Kessler,D.P., Sun,B.I. and Ekker,S.C. (1993) Cooperative binding of an Ultrabithorax homeodomain protein to nearby and distant DNA sites. *Mol. Cell. Biol.*, **13**, 6941–6956.
50. Benson,M. and Pirrotta,V. (1988) The Drosophila zeste protein binds cooperatively to sites in many gene regulatory regions: implications for transvection and gene regulation. *EMBO J.*, **7**, 3907–3915.
51. Ma,X., Yuan,D., Diepold,K., Scarborough,T. and Ma,J. (1996) The Drosophila morphogenetic protein Bicoid binds DNA cooperatively. *Development*, **122**, 1195–1206.
52. Senear,D. and Brenowitz,M. (1991) Determination of binding constants for cooperative site-specific protein-DNA interactions using the gel mobility-shift assay. *J. Biol. Chem.*, **266**, 13661–13671.
53. Burz,D.S., Rivera-Pomar,R., Jackle,H. and Hanes,S.D. (1998) Cooperative DNA-binding by Bicoid provides a mechanism for threshold-dependent gene activation in the Drosophila embryo. *EMBO J.*, **17**, 5998–6009.
54. Hudson,J., Crowe,L. and Fried,M. (1990) A new DNA binding mode for CAP. *J. Biol. Chem.*, **265**, 3219–3225.
55. Beachy,P.A., Krasnow,M.A., Gavis,E.R. and Hogness,D.S. (1988) An Ultrabithorax protein binds sequences near its own and the Antennapedia P1 promoters. *Cell*, **55**, 1069–1081.
56. Schwyter,D., Huang,J., Dubnicoff,T. and Courey,A. (1995) The decapentaplegic core promoter region plays an integral role in the spatial control of transcription. *Mol. Cell. Biol.*, **15**, 3960–3968.
57. Abel,T., Michelson,A.M. and Maniatis,T. (1993) A Drosophila GATA family member that binds to Adh regulatory sequences is expressed in the developing fat body. *Development*, **119**, 623–633.
58. Carey,M., Lin,Y.-S., Green,M.R. and Ptashne,M. (1990) A mechanism for synergistic activation of a mammalian gene by GAL4 derivatives. *Nature*, **345**, 361–364.
59. Lin,Y.-S., Carey,M., Ptashne,M. and Green,M.R. (1990) How different eukaryotic transcriptional activators can cooperate promiscuously. *Nature*, **345**, 359–361.
60. Robe,L.J., Valente,V.L.S., Budnik,M. and Loreto,É.L.S. (2005) Molecular phylogeny of the subgenus Drosophila (Diptera, Drosophilidae) with an emphasis on Neotropical species and groups: a nuclear versus mitochondrial gene approach. *Mol. Phylogenet. Evol.*, **36**, 623–640.
61. Siepel,A., Bejerano,G., Pedersen,J., Hinrichs,A., Hou,M., Rosenbloom,K., Clawson,H., Spieth,J., Hillier,L. and Richards,S. (2005) Evolutionarily conserved elements in vertebrate, insect, worm, and yeast genomes. *Genome Res.*, **15**, 1034–1050.